International Journal of Nanoelectronics and Materials
IJNeaM
ISSN 1985-5761 | E-ISSN 2232-1535

Structural, dielectric, and electrical properties of 3 mol% Ce-doped $BaTiO_3$ ceramics

Ismail Danish Rozaimi [a,b], Rozana Aina Maulat Osman [a,b,d*], Mohd Sobri Idris [b,c], Nurul Izza Mohd Nor [a,d], Nazuhusna Khalid [a,d], Banu Poobalan [a], Zurina Samsudin [e], Yasmin Abdul Wahab [f], Mazlee Mazalan [a,d], and Fadhlina Che Ros [g]

[a]*Faculty of Electronic Engineering Technology, Universiti Malaysia Perlis, 02600, Arau, Perlis, Malaysia*
[b]*Centre of Excellence for Frontier Material Research, Universiti Malaysia Perlis, 02600, Arau, Perlis, Malaysia*
[c]*Faculty of Chemical Engineering Technology, Universiti Malaysia Perlis, 02600, Arau, Perlis, Malaysia*
[d]*Centre of Excellence for Micro System Technology (MiCTEC), Universiti Malaysia Perlis, 02600, Arau, Perlis, Malaysia*
[e]*Fakulti Teknologi Kejuruteraan Industri dan Pembuatan, Universiti Teknikal Malaysia Melaka, Hang Tuah Jaya, 76100, Durian Tunggal, Melaka, Malaysia*
[f]*Nanotechnology & Catalysis Research Centre, University of Malaya, 50603, Kuala Lumpur, Malaysia*
[g]*Pusat Asasi Pertahanan Malaysia, Universiti Pertahanan Malaysia, 50603, Kuala Lumpur, Malaysia*
∗*Corresponding author. Tel.: +60 19-475-7421; e-mail: rozana@unimap.edu.my*

Received 24 November 2024, Revised 19 January 2026, Accepted 29 January 2026

ABSTRACT

The influence of 3 mol% cerium (Ce) in addition to the barium titanate ($BaTiO_3$) on the structural, dielectric, and electrical behavior of $BaTiO_3$ ceramics was examined using samples prepared through the conventional solid-state route. An X-ray diffraction was used to confirm the formation of a pure tetragonal perovskite phase, while a slight reduction in the tolerance factor suggested minor lattice distortion arising from Ce incorporation. From the dielectric measurements, the Curie temperature was shifted to around 60°C, with a high permittivity value of approximately 7267 at 1 kHz, indicating that Ce doping effectively modifies the ferroelectric ordering within the lattice. The Arrhenius plot with an activation energy of 0.49 eV and the temperature-dependent conductivity shows that it may correspond from migration of doubly ionized oxygen vacancies. Impedance analysis shows a semicircular arc, that may correspond to thermally activated relaxation. Result from scanning electron microscopy (SEM) showed well-developed grains with an average size of about 4.26 µm, suggesting Ce-induced grain coarsening beyond its solubility limit. In overall, the aliovalent substitution of Ce^{3+} for Ba^{2+} was found to influence defect chemistry and charge-compensation mechanisms, providing a route to tune both dielectric and electrical characteristics. These findings demonstrate that Ce-doped $BaTiO_3$ offers promising potential as a lead-free ferroelectric material for capacitor and sensor technologies.

Keywords: *Solid state, $BaTiO_3$, Cerium doping, Dielectric properties, Impedance spectroscopy, Ferroelectric ceramics, Microstructure*

1. INTRODUCTION

Dielectric materials are electrical insulators that do not conduct current but can store electrical energy through polarization or known as the effect from the dipole moment. When an external electric field is applied, the positive and negative charges within atoms or molecules shift slightly in opposite directions, forming electric dipoles [1, 2]. Among these materials, ferroelectric ceramics are particularly significant because they exhibit spontaneous electric polarization below a critical temperature known as the Curie temperature (T_c) [3].

Barium titanate ($BaTiO_3$) has been extensively studied for its dielectric piezoelectric, pyroelectric and ferroelectric oxides properties. Due to its high dielectric constant and strong polarization response, $BaTiO_3$ has been widely utilized in multilayer ceramic capacitors (MLCCs) [4, 5], thermistors with a positive temperature coefficient of resistivity (PTCR) [6, 7], actuators, and sensors [8–10]. $BaTiO_3$ serves as a benchmark material for the development of next-generation functional ceramics.

The crystal structure of $BaTiO_3$ belongs to the perovskite family, with the general formula ABX_3, where A and B are cations and X is a non-metallic anion, typically oxygen, forming an ABO_3 framework [11, 12]. This structure exhibits remarkable flexibility, accommodating various distortions and chemical substitutions that allow fine-tuning of its physical properties. While the cubic structure represents the ideal undistorted configuration, $BaTiO_3$ displays several temperature-dependent polymorphs, including tetragonal, orthorhombic, and rhombohedral phases, each associated with distinct orientations of spontaneous polarization. The structural stability can be explained and observed from the Goldschmidt tolerance factor, expressed as Equation (1):

$$t = \frac{R_A + R_O}{\sqrt{2}R_B + R_O} \quad (1)$$

Ideally, the tolerance factor (t) would be t = 1, but in real materials this is rarely the case because t will be defined by the difference of element ionic radii in the A-site radii, R_A, B-site radii, R_B and oxygen radii, R_O in the perovskite structure.

When t differs from 1, the lattice tends to distort through effects such as octahedral tilting, ionic shifts, and lattice strain [13]. These structural changes can modify the crystal symmetry and have a direct impact on the ferroelectric behaviour of $BaTiO_3$, often causing the Curie temperature to shift.

Many researchers have experimented with different dopants to try to improve and adjust the dielectric and ferroelectric behavior of $BaTiO_3$. Among the various elements tested, rare-earth dopants like cerium (Ce) [14, 15] and lanthanum (La) [16, 17] tend to stand out because they can noticeably influence grain growth, defect chemistry, and charge-compensation processes, all of which affect the microstructure and electrical properties of the ceramic. Cerium has been especially interesting to researchers, as it can help stabilize the perovskite structure, change the amount of oxygen vacancies in the lattice, and even lower dielectric loss in some cases.

Despite extensive studies on La-doped $BaTiO_3$, the effects of Ce incorporation, especially its influence on impedance behavior and the differentiation between grain and grain-boundary contributions remain less understood. Therefore, this study examines the effect of 3 mol% Ce incorporation into $BaTiO_3$ ceramics on their dielectric, dielectric loss, and microstructural characteristics. Impedance spectroscopy was employed to analyze the relaxation behavior and to elucidate the relationship between cerium doping, microstructural evolution, and electrical performance.

2. THEORETICAL BACKGROUND

Barium titanate ($BaTiO_3$) is a perovskite-type ceramic that has been widely studied because of its well-known ferroelectric, dielectric, and piezoelectric behavior. Its strong performance mainly comes from its spontaneous polarization [18, 19], which occurs when Ti^{4+} ions shift slightly from the center of the oxygen octahedron in the crystal. This small displacement creates a permanent dipole moment even without an external electric field, which is why $BaTiO_3$ is considered a classic ferroelectric material [20]. When an electric field is applied, this polarization can be switched, producing the familiar hysteresis loop that is important for devices such as capacitors, memory components, and actuators [21].

$BaTiO_3$ exhibits a polymorphic phase transition that are strongly temperature-dependent [22, 23], as illustrated in Figure 1. Above the Curie temperature ($T_m \approx 120°C$), $BaTiO_3$ adopts a cubic paraelectric phase with no net polarization [24]. Upon cooling, it undergoes a sequence of phase transitions from cubic to tetragonal (ferroelectric), then to orthorhombic, and finally to a rhombohedral phase at low temperatures. Each phase is associated with a distinct orientation of the spontaneous polarization vector, imparting $BaTiO_3$ with versatile functional properties across a broad temperature range.

In addition to its ferroelectric and polymorphic behavior, $BaTiO_3$ exhibits a high dielectric constant that peaks near its Curie temperature, making it a key material for multi-layer ceramic capacitors (MLCCs) [25]. The structural stability of $BaTiO_3$ can be rationalized by the Goldschmidt tolerance factor, which describes the geometric compatibility of ions within the perovskite lattice [26]. A decrease in the tolerance factor, typically induced by ionic substitution, enhances lattice distortion, suppresses spontaneous polarization, and consequently lowers the Curie temperature [19, 27]. This correlation between the tolerance factor and ferroelectric behavior underscores the sensitivity of $BaTiO_3$'s properties to compositional modification, providing an effective route for tuning its performance for specific electronic applications.

3. METHODOLOGY

In this study, 3 mol% Ce into barium titanate ($Ba_{0.97}Ce_{0.03}TiO_3$) were synthesized using the solid-state reaction method to investigate microstructural and dielectric properties. The starting materials was barium carbonate ($BaCO_3$), titanium dioxide (TiO_2) and cerium dioxide (CeO_2) from Sigma Aldrich were accurately weighed according to stoichiometric ratios corresponding to each targeted composition. The raw powders were thoroughly mixed using a pestle and mortar adding with acetone to ensure homogenous distribution of solution. The mixed powders were then uniaxially pressed into disk-shaped pellets with 10 mm diameter and a thickness of ~ 1 mm under a pressure of 5 tons.

The pressed pellets were initially subjected to calcination at 1300°C for 6 hours. Subsequently, the pellets sintered in air at 1350°C for 6 hours with heating rates at 5°C/min. To identify the phase formation and crystal structure, sintered pellets was conducted using Bruker D2 Phase X-Ray Diffractometer with Cu-Kα radiation ($\lambda = 1.54$ Å). The diffraction pattern was employed to acquire desired crystalline phases and unveiled any detrimental secondary phases that might compromise the material performance.

Measurement of permittivity with temperature (ε_r–T) was assessed over a temperature range of 5°C to 200°C using an LCR meter (Hioki IM5356). Both surfaces of the sample were coated with silver (Ag) paste as an electrode and fired at 180°C for 30 min. Before applying electrode to the sample, thickness and diameter of the pellet were measured including the weight of pellet. Impedance Spectroscopy (IS) data were modeled with equivalent circuit model using ZView equivalent circuit fitting software.

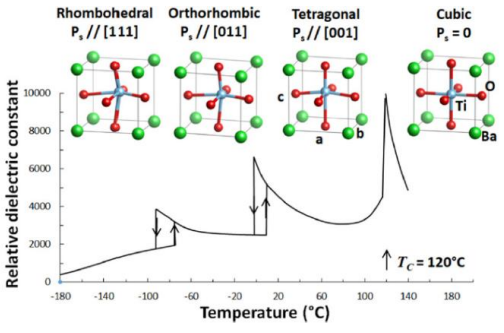

Figure 1. Polymorphism for temperature dependence of Perovskite $BaTiO_3$ [28]

4. RESULTS AND DISCUSSION

4.1. X-Ray Diffraction Analysis

Figure 2 shows the XRD pattern of 3 mol% Ce-doped $BaTiO_3$ sintered at 1350°C for 6 hours. The diffraction scan was collected over the 2θ range of 20–90° with a step size of 0.02°. A monophasic perovskite phase was obtained, with no detectable secondary phases such as CeO_2 [29] or Ba_2TiO_5 [30] in the sample. The clear splitting of the (002) and (200) reflections near $2\theta = 45°$ confirms the tetragonal structure (P4mm), consistent with the PDF card 01-075-1169. The tolerance factor decreased from 1.060 (undoped $BaTiO_3$) [31] to 1.054 (Ce-doped), moving closer to the ideal value of 1. The reduction in tolerance factor indicates a relaxation of lattice distortion within the TiO_6 octahedral network. The resulting decrease in tetragonal distortion leads to a more pseudo-cubic structure which correlates in lowering T_C [32].

4.2. Impedance Spectroscopy Analysis

4.2.1. Dielectric Properties

Temperature dependance of dielectric constant (ε') was recorded in Figure 3 in the range of temperature of 30°C to 200°C at multiple frequencies (10 Hz–100 kHz). The sample showed a sharp, frequency-independent maximum permittivity represents a tetragonal-cubic phase transition occurs at T_C. The maximum permittivity at 1kHz reached a value of 7267 at 60°C indicating that this specimen was found in its ferroelectric state at room temperature. With the introduction of Ce into $BaTiO_3$, the Curie point of undoped $BaTiO_3$ was shifted down to a lower temperature at 60°C as it is in good agreement with reducing tolerance factor leads to a lowering Curie temperature [33].

It is well known, chemical modification of $BaTiO_3$ through A-site aliovalent doping such as this specimen can causes a significant disruption to the ferroelectric domain network of $BaTiO_3$ and therefore results in suppression of T_C with a rate commonly exceeding 10 – 20°C/at. % Dopant [15, 34]. If the substituent cation is Cerium for this case replacing divalent barium, it is termed as a donor-doped as its introduced positive charge termed as $M^{\cdot}_{Ba}$ and will be compensated with cation vacancies (V''_{Ba}, V''''_{Ti}) was refer to [35, 36, 37] in the Equation (2):

$$2Ce_2O_3 + 4Ba_{Ba} + Ti_{Ti} \rightarrow 4M^{\cdot}_{Ba} + V^{''''}_{Ti} + 3BaO + BaTiO_3 \quad (2)$$

Even if Barium vacancies is considered as a charge compensating defects, it is concluded titanium vacancies (V''''_{Ti}) are preferred for donor doped compensation mechanism [38]. However, cerium in general can exists in both trivalent and tetravalent making it a complex element as to interpret a consistent defect mechanism for incorporation into $BaTiO_3$ [39]. Multivalency of Ce can have a caveat though it is tunable element in tailoring to one purpose, trivalent of cerium into has a tendency to occupy the Ba^{2+} site of $BaTiO_3$ lattice; tetravalent will occupy the Ti^{4+} site of $BaTiO_3$. Therefore, site occupancy of cerium lies between the ratio of Ba/Ti [40, 41]. If the ratio is greater than 1, Ce will be preferred to occupy the B-site as Ce^{4+} and for ratio that is lower than 1, Ce have a tendency to occupy the A-site by dominantly become as Ce^{3+} at A-site. Sintering temperature can play a crucial factor on the site occupancy of cerium as Ce^{4+} in CeO_2 slowly changed into Ce^{3+} in Ce_2O_3 [42] corresponding to the reaction in the Equation (3):

$$2CeO_2 \rightarrow Ce_2O_3 + \frac{1}{2}O_2 \quad (3)$$

Figure 4 shows the Arrhenius behavior of log σ in temperature dependence, 1000/T for 3 mol% Ce-doped $BaTiO_3$. The plot was measured at 140°C to 180°C indicating a thermally activated conduction that follows the Arrhenius relation in Equation (4):

$$\sigma = \sigma_o \exp\left(-\frac{E_a}{kT}\right) \quad (4)$$

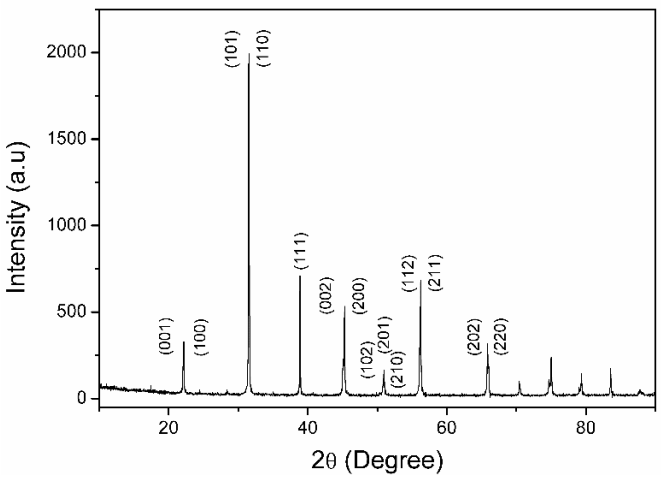

Figure 2. Diffraction pattern of 3 mol% Ce-BT with ICDD 01-075-1169

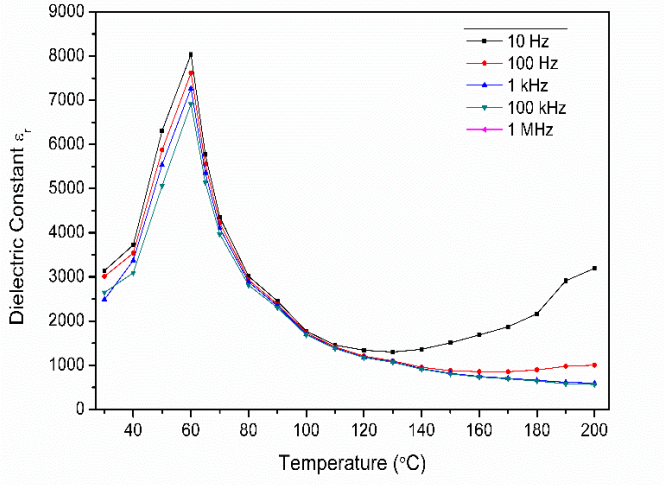

Figure 3. Temperature dependence of dielectric constant of 3 mol% Ce-$BaTiO_3$

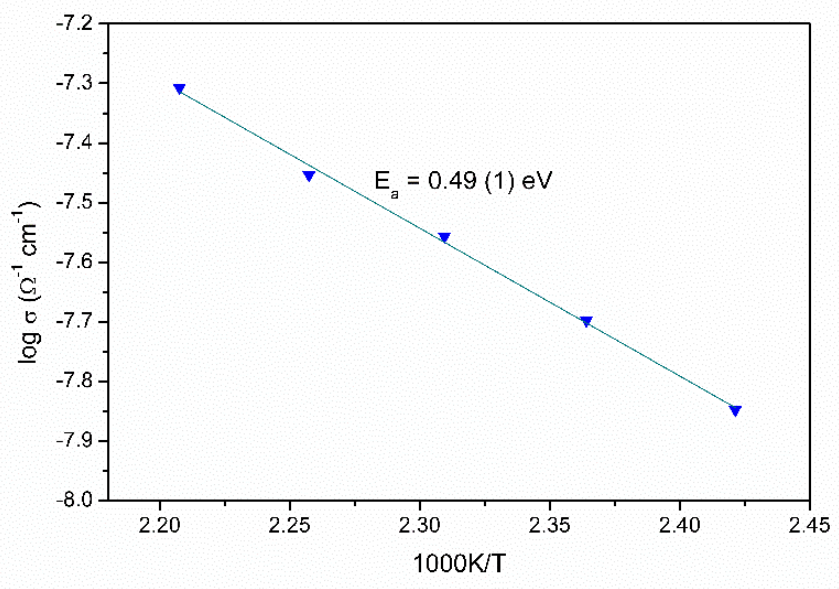

Figure 4. Arrhenius plot of temperature dependance of electric conductivity (170℃ to 190°C)

where σ is the electrical conductivity, σ_o the pre-exponential factor, E_a the activation energy, k the Boltzmann constant, and T the absolute temperature. The activation energy (E_a) of the sample shows a value of 0.49 eV corresponds to the migration of double ionized oxygen vacancies, consistent with donor doped $BaTiO_3$ systems [31]. The introduction of Ce at Ba-site alters the TiO_6 octahedral bond and promotes the formation of compensating oxygen ($V^{\cdot\cdot}_o$) and barium vacancies (V''_{Ba}) [28]. These defects not only facilitate oxygen conduction but also influence grain boundary mobility, where the reduction in pinning centers enables enhanced grain growth at higher concentrations [43].

Figure 5 illustrates the frequency-dependent dielectric loss of 3 mol% Ce-$BaTiO_3$ measured across various temperatures. Dielectric loss represents the fraction of electrical energy dissipated as heat in the material is defined through Equation (5):

$$\tan \delta = \frac{\varepsilon''}{\varepsilon'} \quad (5)$$

where ε" and ε' is the real (energy storage capability) and imaginary (energy dissipation capability) part of permittivity. At low frequencies, dielectric loss is relatively high due to association with Maxwell-Wagner interfacial polarization where charges accumulate at grain boundaries [44]. As the frequency increases, these interfacial charges are unable to follow oscillating field, resulting in a decrease in tan δ up to ~ 10^5 Hz. At higher frequencies the loss rises again which can be related to dipolar relaxation and conduction mechanisms. The increases in dielectric loss at elevated temperature further indicates enhanced conduction process due to thermally activated charges transport.

Figure 6 (a)–(f) present the imaginary parts of impedance (Z") and Modulus (M") spectra for 3 mol% Ce-doped $BaTiO_3$ sample in the temperature range of 30°C to 170°C. At low temperature, both Z" and M" response is broad and shifted toward the low frequency side, indicating strong grain boundary resistance and localized charge carrier motion [45]. At 130°C, the overlap of the Z″ and M″ responses in the low-frequency region indicates that bulk and grain-boundary processes relax on similar timescales, marking the onset of electrical homogeneity. At 150°C, the responses no longer coincide, suggesting partial decoupling of grain-boundary (resistive) and bulk (modulus-dominated) contributions a transitional regime. By 170°C, the Z″ slope again coincides with the low-frequency M″ peak, consistent with reduced grain-boundary resistance and a bulk-dominated, more homogeneous response. This temperature-driven behavior follows an Arrhenius trend consistent with the activation energy obtained at Figure 4. These results confirm that doubly ionized oxygen vacancies govern the transport mechanism.

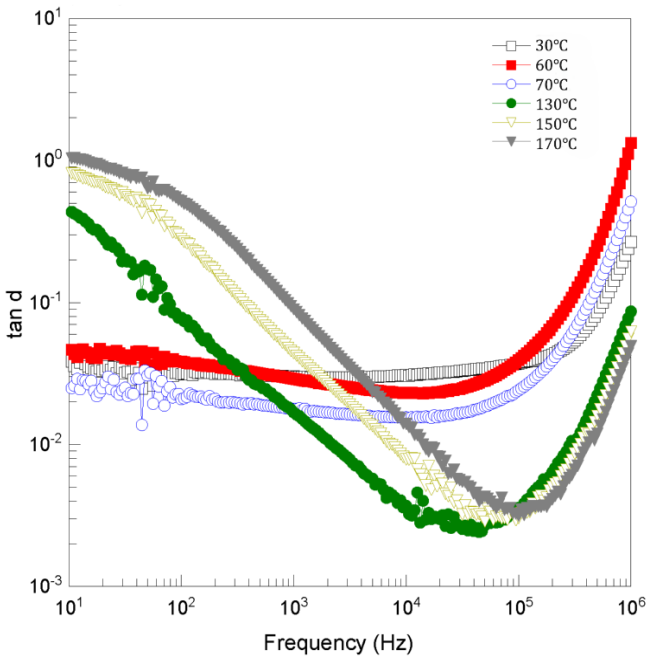

Figure 5. Dielectric loss (tan δ) vs. Frequency (Hz)

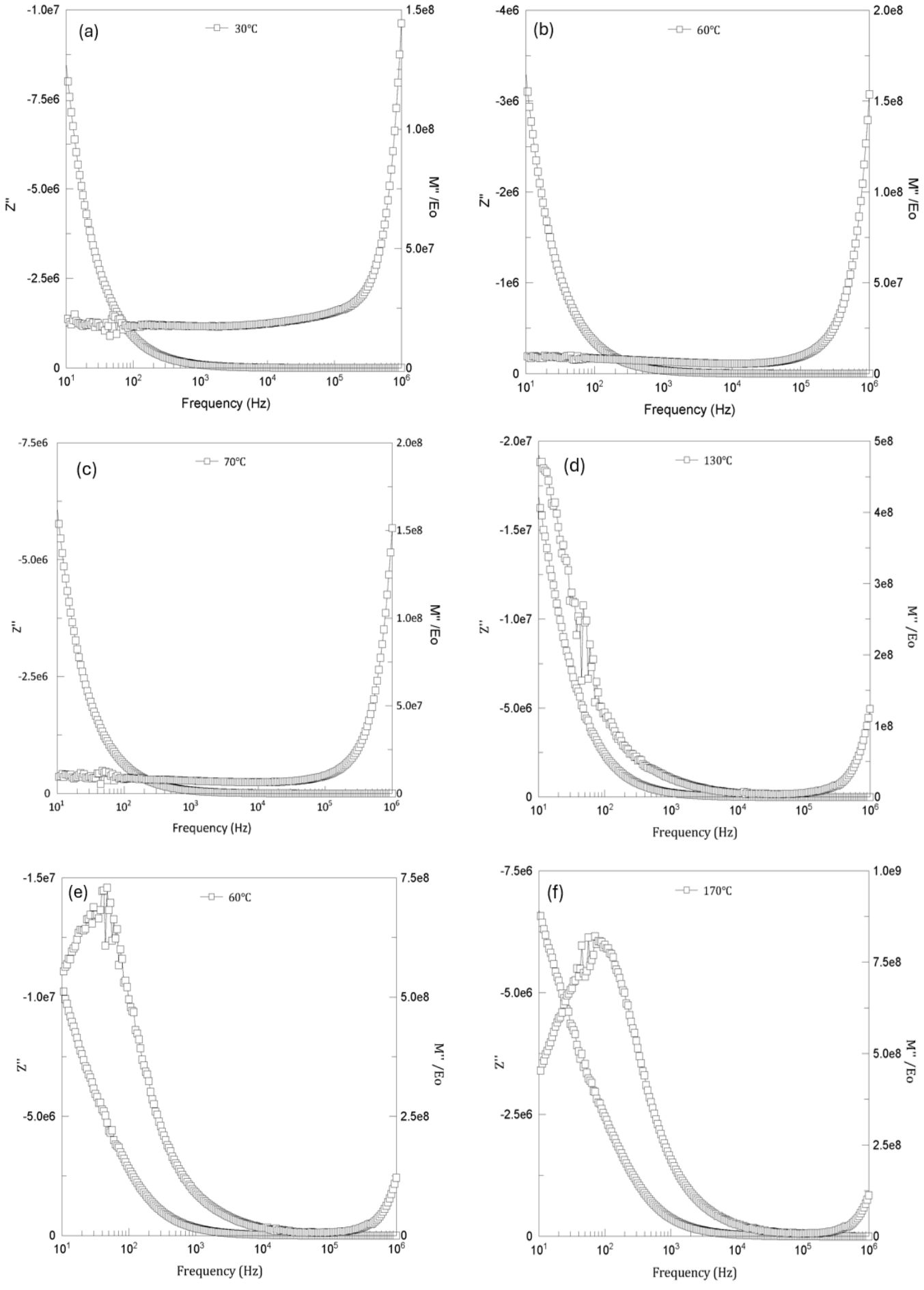

Figure 6. (a–f) Frequency dependence of complex Impedance (Z") – Modulus (M")

Frequency dependent of capacitance for $Ba_{0.97}Ce_{0.03}TiO_3$ ceramic measured at various heating temperature from 30°C to 170°C was displayed in Figure 7. All temperatures exhibit a typical dielectric dispersion behavior, where capacitance decreases with increasing frequency consistent with the characteristics of polarizable dielectric materials. The capacitance reaches a maximum at 60°C and decreases progressively with further heating, attaining the lowest value at 170°C. The temperature sequence in Figure 7 starts from 30°C (square), peaking at 60°C (red square), and reaching a minimum at 170°C (grey triangle). At 1 kHz, the maximum and minimum capacitance values are 4.35×10^{-9} F and 4.23×10^{-10} F, respectively.

The Nyquist plots for 3 mol% Ce-doped $BaTiO_3$ were shown in Figure 8 (a)–(f). At lower temperature (30°C to 70°C), the impedance shows a very high resistance primarily governed by the electrical barriers at the grain boundaries [45]. As temperature rises, the plot reveals a thermally activated conduction process, where the overall complex impedance systematically decreases. This transition to a more conductive state enables the clear resolution of a specific electrical relaxation process, manifesting as a distinct semicircular arc in the plots above 100°C. The diameter of this arc represents the resistance of a specific micro-structural element, also decreases significantly with increasing temperature. This phenomenon highlights the effect of cerium influence acting as a donor dopant element into $BaTiO_3$.

4.3. Microstructural Analysis

Surface morphology of 3 mol% Ce-doped $BaTiO_3$ was displayed in Figure 9 together with the histogram illustrating the grain size distribution of the sample. The histogram of the sample exhibits an average grain size of 4.2645 µm. In general, Ce incorporation into $BaTiO_3$ has been reported to influence the microstructural evolution in a unique manner. At low doping levels (≤ 2 mol%), Ce acts as a donor dopant and typically suppresses grain growth, leading to finer micro-structures. However, when the Ce concentration exceeds ~2 mol %, grain growth is enhanced, and larger grains can form. Literature suggests that the solubility limit of Ce in $BaTiO_3$ is approximately 8 mol% [46], beyond which further doping does not significantly affect the crystal volume or grain size. The average grain size observed in the present sample is consistent with this reported behavior. This evolution in grain size may be related to the defect chemistry arising from Ce doping, where the coexistence of Ce^{3+}/Ce^{4+} states [42] and associated charge compensation mechanisms such as oxygen or cation vacancies [33, 36] can influence grain boundary mobility during sintering.

5. CONCLUSION

The physical, microstructural and electrical analysis of 3 mol% Ce-doped $BaTiO_3$ reveals a close interplay between defect chemistry, grain evolution and charge transport. The dielectric constant shows a shifted T_C to lower temperature of 60°C with maxima permittivity, (ε_{max}) ~7,000 which attributed to Ce^{3+} incorporated into Ba^{2+} site, which reduced tolerance factor of $BaTiO_3$ and disruption of ferroelectric network. Dielectric loss remains stable for low temperature (30°C–70°C) and decreasing tan δ can be seen in the high temperature region (130°C–170°C), but a fluctuation in dielectric loss can be seen across all temperature due to increasing number of vacant in oxygen sites. Overall, the influence of Cerium into $BaTiO_3$ clearly demonstrate the aliovalent doping can be further shifted the Curie temperature to the room temperature while improving maximum permittivity particularly at 0.04 or 0.05 mol Ce concentration [42]. A series of different Ce concentration into $BaTiO_3$ combine the site-selective strategy for this multivalent element can open up a new route as a multifunctional $BaTiO_3$-based materials.

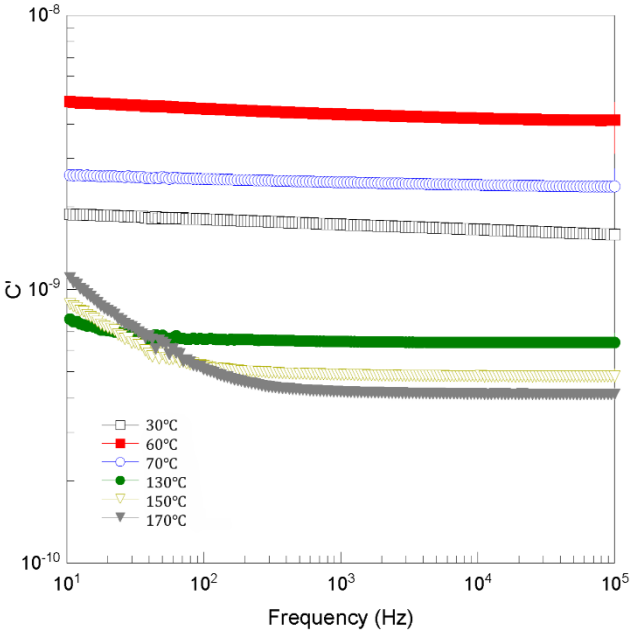

Figure 7. Capacitance of 3 mol% Ce-$BaTiO_3$ at certain temperature

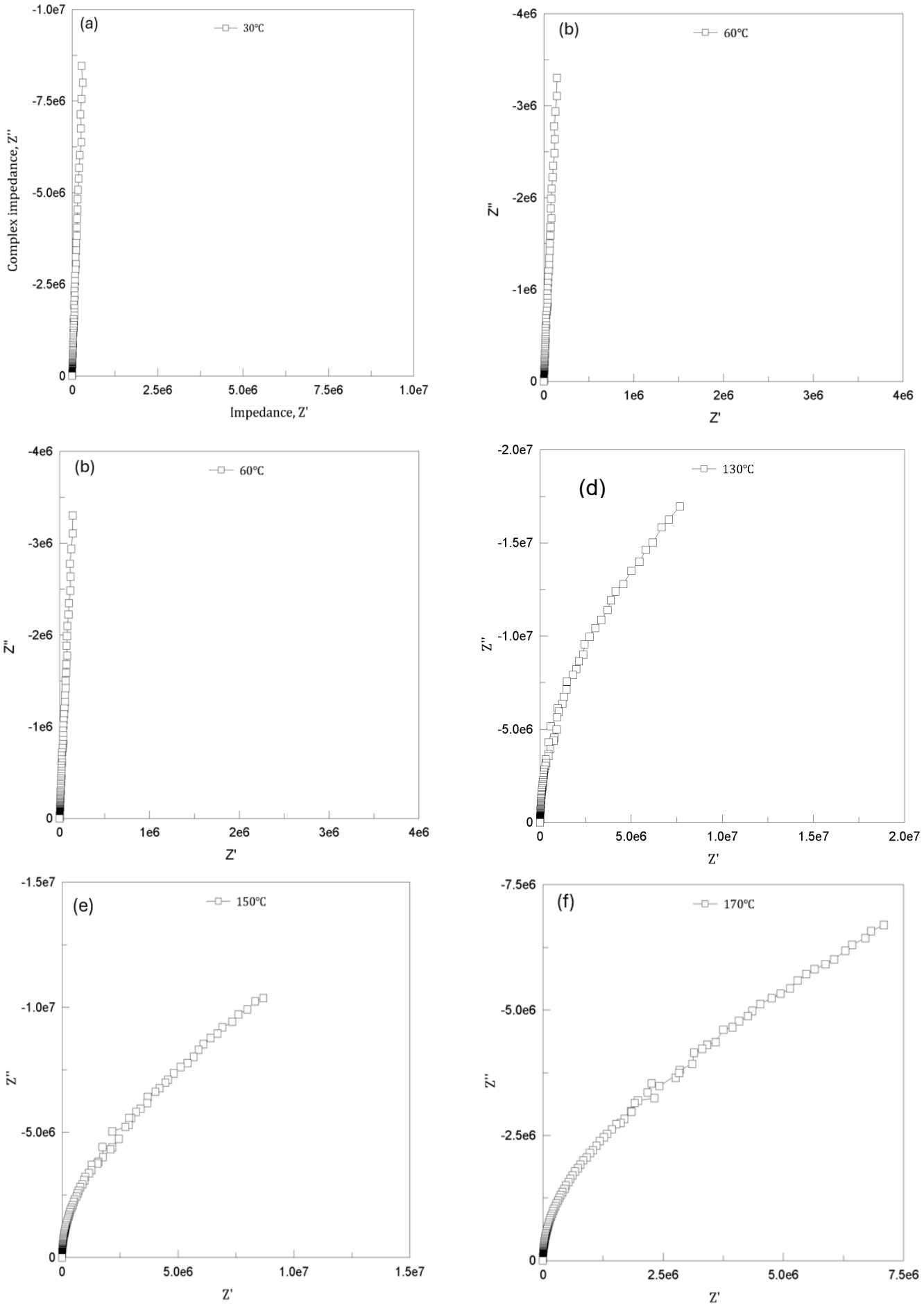

Figure 8. (a–f) Nyquist plot of 3 mol% Ce-$BaTiO_3$ (30°C–170°C)

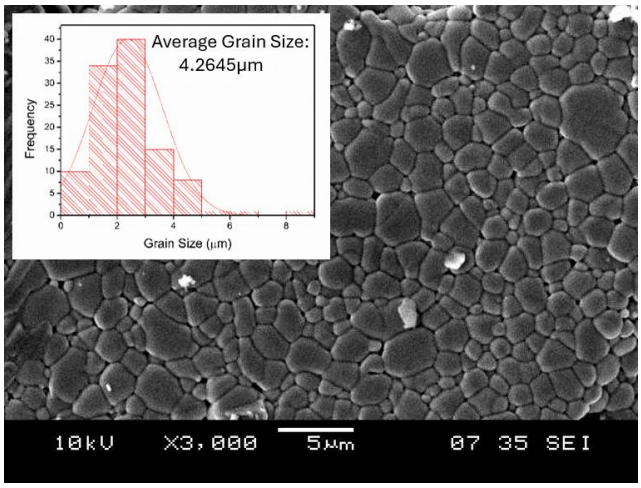

Figure 9. SEM images of $Ba_{0.97}Ce_{0.03}TiO_3$

ACKNOWLEDGMENTS

This work was financially supported by the Ministry of Higher Education Malaysia through the Fundamental ResearchGrant Scheme (FRGS/1/2018/STG07/UNIMAP/02/4) and the MyBrain 2.0 program

REFERENCES

[1] R. Cheng *et al.*, "High-energy-density polymer dielectrics via compositional and structural tailoring for electrical energy storage," *iScience*, vol. 25, no. 8, p. 104837, 2022, doi: 10.1016/j.isci.2022.104837.

[2] N. N. Nasir *et al.*, "Effect of Sn Doping on the Curie Temperature, Structural, Dielectric and Piezoelectric Properties of $Ba_{0.8}Sr_{0.2}Ti_{1-x}Sn_xO_3$ Ceramics," *Journal of Electronic Materials*, vol. 52, no. 11, pp. 7406–7415, 2023, doi: 10.1007/s11664-023-10667-5.

[3] K. N. D. K. Muhsen, R. A. M. Osman, and M. S. Idris, "Colossal permittivity and dielectric behaviour of $(Nb_{0.5}Fe_{0.5})0.1Ti_{0.9}O_2$ and $(Ta_{0.5}Fe_{0.5})0.1Ti_{0.9}O_2$ ceramics," *Journal of Materials Science: Materials in Electronics*, vol. 34, no. 9, p. 777, 2023, doi: 10.1007/s10854-023-10155-w.

[4] Q. Ji, L. Bi, J. Zhang, H. Cao, and X. S. Zhao, "The role of oxygen vacancies of ABO_3 perovskite oxides in the oxygen reduction reaction," *Energy & Environmental Science*, vol. 13, no. 5, pp. 1408–1428, 2020, doi: 10.1039/D0EE00092B.

[5] T. A. T. Sulong, R. A. M. Osman, M. S. Idris, and Z. A. Z. Jamal, "Structural and electrical properties of Barium Titanate ($BaTiO_3$) and Neodymium doped $BaTiO_3$ ($Ba_{0.995}Nd_{0.005}TiO_3$)," *EPJ Web of Conferences*, vol. 162, p. 01050, 2017, doi: 10.1051/epjconf/201716201050.

[6] Y. Chen, "A Combinatorial Method for Discovery of $BaTiO_3$-based Positive Temperature Coefficient Resistors," Thesis, Queen Mary University of London, 2010. Accessed: Dec. 10, 2025. [Online]. Available: https://qmro.qmul.ac.uk/xmlui/handle/123456789/435

[7] T. Plutenko, O. V'yunov, A. Belous, O. Fedorchuk, O. Yanchevskii, and Y. Stupin, "Barium Titanate Based High-Temperature Dielectric Materials Doped with Bismuth, Sodium, Lithium for Metamaterial Application," in *2022 IEEE 41st International Conference on Electronics and Nanotechnology (ELNANO)*, 2022, pp. 87–90. doi: 10.1109/ELNANO54667.2022.9926992.

[8] C. Wang *et al.*, "A general method to synthesize and sinter bulk ceramics in seconds," *Science*, vol. 368, no. 6490, pp. 521–526, 2020, doi: 10.1126/science.aaz7681.

[9] Y. Zhuang *et al.*, "A novel flexible tactile sensor based on Ce-doped $BaTiO_3$ nanofibers," *Semiconductor Science and Technology*, vol. 32, no. 7, p. 074002, 2017, doi: 10.1088/1361-6641/aa6d4b.

[10] E. Aksel and J. L. Jones, "Advances in Lead-Free Piezoelectric Materials for Sensors and Actuators," *Sensors*, vol. 10, no. 3, pp. 1935–1954, 2010, doi: 10.3390/s100301935.

[11] T. A. Colson, M. J. S. Spencer, and I. Yarovsky, "A DFT study of the perovskite and hexagonal phases of $BaTiO_3$," *Computational Materials Science*, vol. 34, no. 2, pp. 157–165, 2005, doi: 10.1016/j.commatsci.2004.12.065.

[12] K. N. D. K. Muhsen, R. A. M. Osman, M. S. Idris, N. I. M. Nadzri, and M. H. H. Jumali, "Effect of sintering temperature on $(Ba_{0.85}Ca_{0.15})$ $(Sn_xZr_{0.1-x}Ti_{0.9})O_3$ for piezoelectric energy harvesting applications," *Ceramics International.*, vol. 47, no. 9, pp. 13107–13117, 2021, doi: 10.1016/j.ceramint.2021.01.175.

[13] L. Lakov, M. Aleksandrova, and V. Blaskov, "Current trends in the development of high dielectric permittivity ceramics," *International Scientific Journal "Materials Science. Non-Equilibrium Phase Transformations"*, vol. 6, no. 1, pp. 8–10, 2020.

[14] R. Sharma *et al.*, "Doping stimulated ferromagnetic ordering and tailoring of the dielectric properties of $Ba_{1-x}Ce_xTiO_3$," *Materials Advances*, vol. 5, no. 21, pp. 8638–8651, 2024, doi: 10.1039/D4MA00593G.

[15] M. A. A. Issa, N. M. Molokhia, and Z. H. Dughaish, "Effect of Cerium Oxide (CeO_2) Additives on the Dielectric Properties of $BaTiO_3$ Ceramics," *Journal of Physics D: Applied Physics*, vol. 16, no. 6, p. 1109, 1983, doi: 10.1088/0022-3727/16/6/019.

[16] T. Y. Zhe, R. A. M. Osman, and M. S. Idris, "Crystal chemistry and electrical properties of La-doped $BaTiO_3$," *AIP Conference Proceedings*, vol. 2347, no. 1, p. 020008, 2021, doi: 10.1063/5.0051868.

[17] F. D. Morrison, D. C. Sinclair, and A. R. West, "Characterization of Lanthanum-Doped Barium Titanate Ceramics Using Impedance Spectroscopy," *Journal of the American Ceramic Society*, vol. 84, no. 3, pp. 531–538, 2001, doi: 10.1111/j.1151-2916.2001.tb00694.x.

[18] G. H. Jaffari, A. ur Rehman, A. M. Iqbal, M. S. Awan, and M. Saleemi, "Extrinsic contributions to the dielectric response in sintered $BaTiO_3$ nanostructures in paraelectric and ferroelectric regimes," *Physica B: Condensed Matter*, vol. 525, pp. 70–77, 2017, doi: 10.1016/j.physb.2017.07.057.

[19] J. Lee, J. Jeong, J. Jung, and H. Jeong, "Optimizing Dielectric Constant in Tetragonal $BaTiO_3$ Via Densification, Tetragonality, and Grain Growth Kinetic with Sintering Temperature," *Archives of*

Metallurgy and Materials, vol. 70, no. No 2, pp. 765–769, 2025, doi: 10.24425/amm.2025.153478.

[20] D. Zorin *et al.*, "Effects of mechanical activation on the formation process of ferroelectric piezoelectric ceramics," *Journal of Electroceramics*, 2025, doi: 10.1007/s10832-025-00417-w.

[21] A. Kang, L. Li, X. Deng, and X. Wang, "The study on high temperature conductivity of nanocrystalline $BaTiO_3$ ceramics," *Materials Science and Engineering: B*, vol. 132, no. 3, pp. 288–291, 2006, doi: 10.1016/j.mseb.2006.04.031.

[22] N. H. Yusoff, R. A. M. Osman, M. S. Idris, K. N. D. K. Muhsen, and N. I. M. Nor, "Dielectric and structural analysis of hexagonal and tetragonal phase $BaTiO_3$," *AIP Conference Proceedings*, vol. 2203, p. 020038, 2020, doi: 10.1063/1.5142130.

[23] D. Li *et al.*, "Progress and perspectives in dielectric energy storage ceramics," *Journal of Advanced Ceramics*, vol. 10, no. 4, pp. 675–703, 2021, doi: 10.1007/s40145-021-0500-3.

[24] N. Iqbal, A. Dixit, P. S. Dobal, R. S. Katiyar, and A. S. Bhalla, "Doping effects in barium titanate: a historical perspective and review," *Journal of Materials Science: Materials in Electronics*, vol. 36, no. 16, p. 1008, 2025, doi: 10.1007/s10854-025-15032-2.

[25] K. Laadjal and A. J. M. Cardoso, "Multilayer Ceramic Capacitors: An Overview of Failure Mechanisms, Perspectives, and Challenges," *Electronics*, vol. 12, no. 6, p. 1297, 2023, doi: 10.3390/electronics12061297.

[26] M.-J. Pan and C. A. Randall, "A brief introduction to ceramic capacitors," *IEEE Electrical Insulation Magazine*, vol. 26, no. 3, pp. 44–50, 2010, doi: 10.1109/MEI.2010.5482787.

[27] M. P. Hautzinger, W. Mihalyi-Koch, and S. Jin, "A-Site Cation Chemistry in Halide Perovskites," *Chemistry of Materials*, vol. 36, no. 21, pp. 10408–10420, 2024, doi: 10.1021/acs.chemmater.4c02043.

[28] V. Buscaglia, M. T. Buscaglia, and G. Canu, "$BaTiO_3$-Based Ceramics: Fundamentals, Properties and Applications," in *Encyclopedia of Materials: Technical Ceramics and Glasses*, Elsevier, 2021, pp. 311–344. doi: 10.1016/B978-0-12-803581-8.12132-0.

[29] J. H. Hwang and Y. H. Han, "Electrical Properties of Cerium-Doped $BaTiO_3$," *Journal of the American Ceramic Society*, vol. 84, no. 8, pp. 1750–1754, 2001, doi: 10.1111/j.1151-2916.2001.tb00910.x.

[30] Sabina Yasmin, S. Choudhury, M. A. Hakim, A. H. Bhuiyan, and M. J. Rahman, "Effect of Cerium Doping on Microstructure and Dielectric Properties of $BaTiO_3$ Ceramics," *Journal of Materials Science & Technology*, vol. 27, no. 8, pp. 759–763, 2011, doi: 10.1016/S1005-0302(11)60139-4.

[31] Y. Huang, C. Zhao, S. Zhong, and J. Wu, "Highly Tunable Multifunctional $BaTiO_3$-Based Ferroelectrics via Site Selective Doping Strategy," *Acta Materialia*, vol. 209, p. 116792, 2021, doi: 10.1016/j.actamat.2021.116792.

[32] Mahmoud. S. Alkathy, H. A. Kassim, K. G. Mansour, J. P. Goud, and J. A. Eiras, "Achieving superior energy storage performance in barium titanate ceramics via a rare earth co-doping strategy," *Ceramics - Silikaty*, pp. 505–515, 2024, doi: 10.13168/cs.2024.0049.

[33] S. Liu, L. Zhang, J. Wang, Y. Zhao, and X. Wang, "Abnormal Curie temperature behavior and enhanced strain property by controlling substitution site of Ce ions in $BaTiO_3$ ceramics," *Ceramics International*, vol. 43, no. 14, pp. 10683–10690, 2017, doi: 10.1016/j.ceramint.2017.04.164.

[34] T. Nakagawa, M. Menelaou, and M. Vrankić, "Showcasing the Structure and Properties of Lanthanide-Doped $BaTiO_3$," *Advanced Physics Research*, vol. 4, no. 9, p. 2500006, 2025, doi: 10.1002/apxr.202500006.

[35] Z. Hasan *et al.*, "Effect of Ce doping on the multifunctional properties of $BaTiO_3$: From bandgap engineering to mechanical stability," *Next Materials*, vol. 9, p. 101133, 2025, doi: 10.1016/j.nxmate.2025.101133.

[36] Z.-K. Han, W. Liu, and Y. Gao, "Advancing the Understanding of Oxygen Vacancies in Ceria: Insights into Their Formation, Behavior, and Catalytic Roles," *JACS Au*, vol. 5, no. 4, pp. 1549–1569, 2025, doi: 10.1021/jacsau.5c00095.

[37] K. Zhang, L. Li, M. Wang, and W. Luo, "Charge compensation in rare earth doped $BaTiO_3$-based ceramics sintered in reducing atmosphere," *Ceramics International*, vol. 46, no. 16, Part A, pp. 25881–25887, 2020, doi: 10.1016/j.ceramint.2020.07.072.

[38] D.-Y. Lu, X.-Y. Sun, and M. Toda, "A novel high-k 'Y5V' barium titanate ceramics co-doped with lanthanum and cerium," *Journal of Physics and Chemistry of Solids*, vol. 68, no. 4, pp. 650–664, 2007, doi: 10.1016/j.jpcs.2007.02.018.

[39] Y. A. Zulueta, T. C. Lim, and J. A. Dawson, "Defect Clustering in Rare-Earth-Doped $BaTiO_3$ and $SrTiO_3$ and Its Influence on Dopant Incorporation," *The Journal of Physical Chemistry C*, vol. 121, no. 42, pp. 23642–23648, 2017, doi: 10.1021/acs.jpcc.7b08500.

[40] M. T. Buscaglia, V. Buscaglia, M. Viviani, and P. Nanni, "Atomistic Simulation of Dopant Incorporation in Barium Titanate," *Journal of the American Ceramic Society*, vol. 84, no. 2, pp. 376–84, 2001, doi: 10.1111/j.1151-2916.2001.tb00665.x.

[41] J. H. Hwang and Y. H. Han, "Dielectric Properties of $(Ba_{1-x}Ce_x)TiO_3$," *Japanese Journal of Applied Physics*, vol. 39, no. 5R, p. 2701, 2000, doi: 10.1143/JJAP.39.2701.

[42] D. F. K. Hennings, B. Schreinemacher, and H. Schreinemacher, "High-permittivity dielectric ceramics with high endurance," *Journal of the European Ceramic Society*, vol. 13, no. 1, pp. 81–88, 1994, doi: 10.1016/0955-2219(94)90062-0.

[43] W. Preis, A. Burgermeister, W. Sitte, and P. Supancic, "Bulk and grain boundary resistivities of donor-doped barium titanate ceramics," *Solid State Ionics*, vol. 173, no. 1–4, pp. 69–75, 2004, doi: 10.1016/j.ssi.2004.07.054.

[44] L. P. Curecheriu, C. E. Ciomaga, V. Musteata, G. Canu, V. Buscaglia, and L. Mitoseriu, "Diffuse phase transition and high electric field properties of $BaCe_yTi_{1-y}O_3$ relaxor ferroelectric ceramics," *Ceramics International*, vol. 42, no. 9, pp. 11085–11092, 2016, doi: 10.1016/j.ceramint.2016.04.008.

[45] A. R. Albuquerque, A. Bruix, I. M. G. Dos Santos, J. R. Sambrano, and F. Illas, "DFT Study on Ce-Doped Anatase TiO_2 : Nature of Ce^{3+} and Ti^{3+} Centers Triggered by Oxygen Vacancy Formation," *The Journal of Physical Chemistry C*, vol. 118, no. 18, pp. 9677–9689, 2014, doi: 10.1021/jp501757f.

[46] D. Makovec, Z. Samardžija, and D. Kolar, "Solid Solubility of Cerium in $BaTiO_3$," *Journal of Solid State Chemistry*, vol. 123, no. 1, pp. 30–38, 1996, doi: 10.1006/jssc.1996.0148.